

F. W. OHRENDORF, H. HAEUSELER

Laboratorium für Anorganische Chemie, Universität Siegen, Germany

Lattice Dynamics of Chalcopyrite Type Compounds. Part II. Calculations in a Short Range Force Field Model

The lattice dynamics of 12 chalcopyrite type compounds CuAlS_2 , CuGaS_2 , CuInS_2 , AgGaS_2 , AgGaSe_2 , AgInSe_2 , ZnSiP_2 , ZnGeP_2 , CdSiP_2 , CdGeP_2 , CdSnP_2 , and CdGeAs_2 have been investigated based on 4 different short range force constant models. In all models a set of different solutions can be obtained which can be distinguished by their force constant patterns. For a comparison of the calculated force constants it is therefore necessary to use the data of the comparable minima. From the set of solutions one is selected by physical reasoning and complete results for a model with 8 force constants are given for this minimum for all 12 compounds. The calculated force constants, normal co-ordinates and potential energy distributions are compiled and discussed.

Keywords: chalcopyrite, lattice dynamics, force constants, short range model

Introduction

A large number of lattice dynamical calculations on chalcopyrite type compounds is reported in the literature, which are not directly comparable as they are done on the basis of different models, i.e. the calculations in a Urey-Bradley-force-field-model by LAUWERS and HERMAN, in modified Keating models by NEUMANN, KOSCHEL and BETTINI, in a rigid-ion-model by POPLAVNOI and TYUTEREV as well as by KOPYTOV and POPLAVNOI, and different sets of short range force constants. For a better understanding of the lattice dynamics of this group of compounds we started calculations with a short range model and a rigid ion model for a large group of chalcopyrites, both chalcogenides and pnictides. In part I of this series of papers we gave a critical evaluation of the vibrational frequencies found in the literature for chalcopyrite type compounds. In this paper we will give our results on the lattice dynamics of chalcopyrite type compounds on the basis of a short range force field model using Wilson's GF-matrix method.

Structure Data, Symmetry Co-ordinates, and Phonon Frequencies

Chalcopyrites ABX_2 crystallise in the space group $\overline{\text{I}}42\text{d} - \text{D}_{2\text{d}}^{12}$ with four formula units in the unit cell, i.e. two formula units in the primitive cell. The unit cell of the chalcopyrite structure is shown in fig.1. Structural data for the chalcopyrites under discussion are given in table I. Group theoretical treatment of the optical phonons at the zone centre results in following irreducible representation:

$$\Gamma = A_1(\text{Ra}) + 2A_2 + 3B_1(\text{Ra}) + 3B_2(\text{IR, Ra}) + 6E(\text{IR, Ra})$$

The symmetry co-ordinates of the Raman and IR-allowed modes are listed in table II. They agree with those given in the literature by KAMINOV et al. and HOLAH et al. in most parts. The main differences are due to a different numbering of the atoms of the primitive cell (see fig.1). The vibrational frequencies of the optical phonon modes are given in our previous paper (OHRENDORF and HAEUSELER).

compound	literature	structure parameters				bond distances	
		a	c	x	V	AX	BX
CuAlS ₂	SPIES et al.	533.4	1044	0.275	149	237.6	221.9
CuGaS ₂	SPIES et al.	535.6	1044	0.276	150	238.2	222.3
CuInS ₂	SPIES et al.	552.3	1112	0.215	170	229.0	251.5
AgGaS ₂	SPIES et al.	575.4	1030	0.305	171	260.7	223.4
AgGaSe ₂	SPIES et al.	598.5	1073	0.276	192	260.2	241.5
AgInSe ₂	BENOIT et al.	610.4	1171	0.259	218	263.8	257.8
ZnSiP ₂	ABRAHAMS et al. (1970)	539.9	1044	0.269	152	237.4	225.3
ZnGeP ₂	VAIPOLIN	546.5	1070	0.267	160	240.5	229.7
CdSiP ₂	ABRAHAMS et al. (1971)	568.0	1043	0.297	168	256.1	224.7
CdGeP ₂	VAIPOLIN	574.0	1078	0.283	178	255.2	232.9
CdSnP ₂	VAIPOLIN	590.1	1151	0.265	200	258.7	248.4
CdGeAs ₂	VAIPOLIN	594.3	1122	0.279	198	262.9	243.0

Table I: Lattice parameters a/pm and c/pm , volume of the unit cell $V \cdot 10^{-6}/\text{pm}^3$, positional parameter x of the anion and bond distances AX/pm and BX/pm for chalcopyrites ABX_2 .

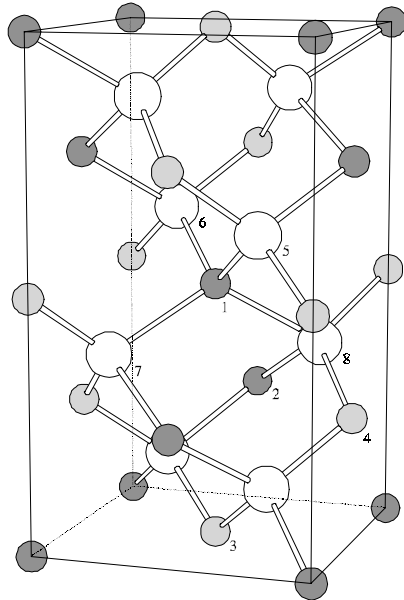


Fig.1: Unit cell of the chalcopyrite lattice (large circles: anions, dark grey: A-cations, light grey: B-cations)

species	short-cut	symmetry co-ordinate
A ₁	SC1	$y_5 - y_6 + x_7 - x_8$
A ₂	SC2	$-x_5 + x_6 + y_7 - y_8$
	SC3	$z_5 + z_6 - z_7 - z_8$
B ₁	SC4	$z_1 - z_2$
	SC5	$z_3 - z_4$
	SC6	$-y_5 + y_6 + x_7 - x_8$
B ₂	SC7	$z_1 + z_2$
	SC8	$z_3 + z_4$
	SC9	$z_5 + z_6 + z_7 + z_8$
	SC10	$-x_5 + x_6 - y_7 + y_8$
E	SC11	$x_1 + x_2 + y_1 + y_2$
	SC12	$x_3 + x_4 + y_3 + y_4$
	SC13	$x_5 + x_6 + y_7 + y_8 + y_5 + y_6 + x_7 + x_8$
	SC14	$z_5 - z_6 + z_7 - z_8$
	SC15	$x_1 - x_2 - y_1 + y_2$
	SC16	$x_3 - x_4 - y_3 + y_4$
	SC17	$x_5 + x_6 + y_7 + y_8 - y_5 - y_6 - x_7 - x_8$

Table II: Symmetry co-ordinates for the chalcopyrite lattice

Potential Models

For the description of the potential energy of the chalcopyrite lattice we used the following force constants: two valence force constants K1 and K2 for the interaction of the two metal ions occupying different crystallographic sites with their nearest anion neighbours. Force constants between next nearest neighbours are F11, F12, F21, and F22 for anion-anion interaction, F31 for A-A and F32 for B-B interaction and F33 and F34 for the two different A-B interactions. Components of the vibrations perpendicular to the valence forces we describe by the angle deformation force constants H11 and H12 for the two different angles at the A-atom, H21 and H22 with atom B as a vertex, and H41, H42, H43, and H44 with an X-atom as a vertex. Furthermore there is one interaction constant k for the interaction of the internal co-ordinates A-X and B-X. A compilation of the different force constants, the corresponding internal co-ordinates and the interatomic distances and angles obtained from single crystal structure determinations is given in table III.

From these 19 internal co-ordinates we built three different force constant models SR I, SR II, and SR III with 11 force constants each. Common to all three of them are K1, K2 and k. Besides these three constants the model SR I includes the 8 next nearest neighbour interactions while in SR II the next nearest neighbour interactions are modelled by deformation force constants. The model SR III uses as well next nearest neighbour interactions as deformation constants. Though the angles and distances around the tetrahedrally coordinated cations are not equal due to the tetragonal distortion of the lattice we introduced the following constraints to fix the number of variable constants to 11: $F_{11}=F_{12}=F_{21}=F_{22}=F_2$, $F_{33}=F_{34}$, $H_{11}=H_{12}=H_1$, $H_{21}=H_{22}=H_2$, and $H_{31}=H_{32}=H_{33}=H_{34}=H_3$.

Internal co-ordinates	Distances /pm angles /°	models			
		SR I	SR II	SR III	SR IV
8 KAX	237	K1	K1	K1	K1
8 KBX	223	K2	K2	K2	K2
4 H _{XAX} ^z	113.0	-	H11	H1	-
8 H _{XAX} ^{xy}	107.7	-	H12		
4 H _{XBX} ^z	108.2	-	H21	H2	H2
8 H _{XBX} ^{xy}	110.1	-	H22		
4 F _{XAX} ^{xy}	396	F11	-	F1	F1
8 F _{XAX} ^{xyz}	383	F12	-		
4 F _{XBX} ^{xy}	362	F21	-	F2	
8 F _{XBX} ^{xyz}	366	F22	-		
4 FAA	374	F31	-	F31	F31
4 FBB	374	F32	-	F32	F32
8 F _{AB} ^{xy}	378	F33	-	F33	F33
8 F _{AB} ^{xyz}	374	F34	-		
4 H _{AXA}	104.2	-	H31	H3	-
4 H _{BXB}	113.9	-	H32		
8 H _{AXB} ^z	110.4	-	H33		
8 H _{AXB} ^{xy}	108.7	-	H34		
16 k _{AXBX}		k	k	k	k

Table III: Internal co-ordinates and corresponding force constants for chalcopyrites ABX₂ used in 4 different short range force constant models.

Calculations

The force constant calculations have been performed with a modified version of Shimanouchi's program LXSM written in Pascal for an IBM compatible computer by OHRENDORF. The force constants were varied in order to minimise the function

$$\Delta F = \sqrt{\sum W_i (FRQ_i - FRC_i)^2 / \sum W_i}$$

where FRQ_i are the observed and FRC_i the calculated frequencies and W_i the corresponding weights.

The observed frequencies used in our calculations are those which we think are reliable according to our previous paper (OHRENDORF and HAEUSELER) completed in the case of missing frequencies of species B₁ by estimated values. For these estimated frequencies, set in italics in tables VII and VIII, we set the weights to W_i = 0.5 while all the other frequencies are weighted by W_i = 1.0.

For all three models we found a variety of minima with all compounds under investigation which can be distinguished by the pattern of the values of the force constants: minimum M1 with K1 < K2, minimum M2 with K1 > K2, M3 with K1 ≈ 0, and M4 with K2 ≈ 0. All these minima are further split due to the values of the metal-metal interactions. In the minima of type A the interaction of the A-cations is predominant and for type B that of the B-cations. Typical values obtained with the force constant model SR III are shown in table IV and V for CuGaS₂ (for the results obtained with the other models and for the other compounds see OHRENDORF). These minima are found for all compounds under investigation.

modes	observed	Frequencies (cm ⁻¹)							
		calculated in minimum							
		M1A ΔF=1.7	M1B ΔF=1.3	M2B ΔF=1.9	M2A ΔF=1.3	M3B ΔF=4.1	M4A ΔF=4.2	M1B' ΔF=2.8	M2A' ΔF=2.6
A ₁	312	315.5	312.3	315.4	311.7	318.9	320.0	315.4	314.9
A ₂	-	347.9	345.6	346.4	344.4	331.0	340.3	326.8	325.6
A ₂	-	277.2	283.1	278.9	284.7	301.7	311.2	294.8	299.2
B ₁ ¹	358	355.6	359.8	355.1	359.2	353.4	354.8	354.1	355.1
B ₁ ²	203	202.9	201.5	202.7	201.9	202.4	201.9	204.0	202.8
B ₁ ³	97	96.8	97.0	96.8	95.9	99.7	96.9	97.4	95.7
B ₂ ¹	368	368.8	369.7	368.0	368.8	372.3	377.9	370.9	370.5
B ₂ ²	262	262.7	263.4	263.1	263.2	262.6	260.2	265.1	265.2
B ₂ ³	95	93.9	94.1	94.8	92.7	96.7	94.0	95.2	95.7
B ₂ ⁴	0	0.0	0.0	0.0	0.0	0.0	0.0	0.0	0.0
E ¹	363	361.6	362.0	361.6	364.1	357.1	359.2	358.1	358.7
E ²	332	334.1	330.9	334.9	331.6	330.5	329.2	333.7	334.9
E ³	262	260.7	260.7	259.8	260.9	255.5	257.4	258.2	258.5
E ⁴	156	158.1	157.9	158.0	157.7	159.9	160.2	154.8	156.3
E ⁵	-	107.7	103.4	108.9	103.5	107.6	105.2	102.7	102.3
E ⁶	74	73.6	74.5	73.9	74.7	71.6	72.6	74.1	75.4
E ⁷	0	0.0	0.0	0.0	0.0	0.0	0.0	0.0	0.0

Table IV: Observed and in different minima of model SR III calculated frequencies FRC (cm⁻¹) for CuGaS₂

In most cases, but not in all, M1B and M2A lead to a better agreement between observed and calculated frequencies than M1A and M2B. As it is more reasonable that K1 which describes the interaction of the metal ion of lower formal charge with the anion is smaller than K2 where the cation of higher formal charge is involved, we prefer the solution in M1 over that in M2. Furthermore this choice is supported by the unreasonable result that for the minimum M2 in both series CuBS₂ (B=Al,Ga,In) and CdBP₂ (B=Si,Ge,Sn) the force constants K1 decrease with increasing mass of the B-cation from 1.8 to 1.2 to 0.8 and from 2.5 to 1.6 to 1.1 N/cm, respectively, while K2 exhibits only minor changes (for details see OHRENDORF).

From the solutions of type A and B we prefer the minimum M1B over M1A because in M1A we find unusual high values for the interaction of the A-metal ions of up to 1.6 N/cm for CdSiP₂, i.e. for compounds with a B-cation of small mass, and 0.14 N/cm for CuInS₂, i.e. for compounds with a cation of high mass. For the following calculations we therefore present the results in minimum M1B only. The influence of the potential models on the results of the calculations is shown in table VI on CuGaS₂ as an example. On an average, all three models deliver relatively good descriptions of the spectra, the error being around 5 cm⁻¹, i.e. similar to the experimental error of the experimental frequencies. Equal to all three models is the difficulty in the description of the modes of species B₁, which exhibit relatively large deviations between the observed frequencies (though they show relatively

large experimental uncertainties) and the calculated ones in comparison with the other modes. Similar problems are found for the modes E^1 and E^2 which for all compounds lie in value closer to each other in the experimental data than in the calculated. This problem is minimal for the model SR III, which therefore leads to better results.

Min.	ΔF	K1	K2	H1	H2	H4	F1	F2	F31	F32	F33	k
M1A	1.7	0.503	1.144	0.005	0.026	0.001	0.099	0.102	0.283	-0.125	-0.023	-0.051
M1B	1.3	0.506	1.134	0.020	0.016	0.002	0.124	0.080	-0.044	0.283	-0.040	-0.032
M2B	1.9	1.122	0.502	0.023	0.009	0.002	0.107	0.100	-0.121	0.306	-0.026	-0.042
M2A	1.3	1.120	0.506	0.011	0.018	0.006	0.086	0.121	0.254	-0.044	-0.040	-0.019
M3B	4.1	0.245	1.015	0.009	0.046	0.053	0.183	0.003	-0.020	0.153	-0.066	-0.066
M4A	4.2	1.022	0.179	0.049	0.008	0.047	0.001	0.235	0.095	-0.001	-0.048	-0.040
M1B'	2.8	0.328	1.039	0.016	0.036	0.049	0.155	0.001	-0.040	0.206	-0.084	-0.067
M2A'	2.6	1.030	0.310	0.042	0.010	0.045	0.002	0.169	0.153	-0.026	-0.071	-0.061

Table V: Force constants in N/cm and error ΔF in cm^{-1} for CuGaS_2 in different minima of the potential model SR III

mode	frequencies			
	observed	calculated by model		
		SR I ($\Delta F=2.2$)	SR II ($\Delta F=5.0$)	SR III ($\Delta F=1.3$)
A_1	312	312.9	312.5	311.6
A_2		331.7	306.5	343.4
A_2		284.0	234.9	283.7
B_1^1	358	358.7	353.9	359.1
B_1^2	203	200.3	196.2	202.2
B_1^3	97	98.2	99.8	96.0
$B_{2\text{TO}}^1$	368	367.5	373.2	369.1
$B_{2\text{TO}}^2$	262	257.9	269.9	262.6
$B_{2\text{TO}}^3$	95	96.7	94.0	92.6
E_{TO}^1	363	362.6	372.1	361.0
E_{TO}^2	332	331.8	327.6	330.6
E_{TO}^3	262	264.3	255.9	260.8
E_{TO}^4	156	160.4	157.7	157.3
E_{TO}^5	-	99.3	123.6	102.1
E_{TO}^6	74	72.1	73.1	74.5

Table VI: Observed and with the potential models SR I, SR II, and SR III calculated frequencies for CuGaS_2 (in cm^{-1})

As one problem of the calculations arises from the rather broad and flat minima which lead to relatively large uncertainties in the obtained force constants and as this in part is due to the high number of parameters compared to the number of experimental frequencies, we further reduced the number of independent force constants in the model SR IV from 11 to 8 by introducing additional constraints between the force constants of model SR III which were derived from the results of our calculations obtained for the other models: $F1 = F2$, $H1 = 0$, and $H3 = 0$. This model exhibits the same properties as the model SR III but due to the constrains between the force constants used it shows the minima M1 and M3 only.

Results

For the final calculations on 12 compounds with chalcopyrite structure we used the model SR IV derived from model SR III. The results of these calculations obtained in the minimum M1 are compiled in table VII and VIII. With a mean deviation of 4cm^{-1} the results obtained with SR IV are not significantly worse than those obtained with model SR III.

As can be seen from table VII the mean quadratic deviation ΔF between experimental and calculated frequencies is in the same order of magnitude as the experimental error for the vibrational frequencies. A comparison of the deviations obtained for the corresponding modes of all 12 compounds shows that also in this case the mean values are in the same order of magnitude as the experimental error, i.e. the frequencies of all the modes are fitted equally good. But especially the modes of species B_1 and B_2 exhibit deviations which are located on the upper border of this range. The mean values of the deviations for the different modes on the other hand show that for instance calculated frequencies of the modes B_1^1 and

ΔF	CuAlS ₂		CuGaS ₂		CuInS ₂		AgGaS ₂		AgGaSe ₂		AgInSe ₂	
	FRQ	FRC	FRQ	FRC	FRQ	FRC	FRQ	FRC	FRQ	FRC	FRQ	FRC
A ₁	315	314.2	312	313.1	294	290.4	295	289.7	181	175.1	172	171.4
A ₂		341.0		345.8		319.1		333.6		177.3		184.0
A ₂		277.9		280.5		254.2		233.5		148.4		145.7
B ₁ ¹	443	450.6	358	358.9	<i>309</i>	318.0	334	339.4	253	257.2	<i>214</i>	215.6
B ₁ ²	268	260.7	203	202.6	<i>162</i>	157.1	190	189.0	160	153.3	<i>123</i>	126.2
B ₁ ³	98	98.5	97	100.6	83	104.0	54	54.6	58	54.5	<i>50</i>	52.6
B ₂ ¹	446	447.2	368	366.8	323	322.7	367	367.7	252	248.6	208	209.0
B ₂ ²	271	278.4	262	263.5	234	241.2	212	220.1	155	165.5	149	150.3
B ₂ ³	112	120.8	95	96.4	79	77.2	65	60.9	58	65.9	41	41.1
B ₂ ⁴	0	0.0	0	0.0	0	0.0	0	0.0	0	0.0	0	0.0
E ¹	444	443.0	363	364.0	321	323.8	368	368.6	255	254.8	215	214.7
E ²	432	424.3	332	330.7	295	293.0	325	322.1	251	254.8	200	198.2
E ³	263	259.5	262	259.3	244	240.5	226	220.1	162	160.0	153	152.8
E ⁴	216	216.7	165	166.1	140	134.4	157	159.3	137	134.7	106	104.1
E ⁵	137	135.6	115	112.4	88	90.3	95	85.1	84	81.6	60	59.6
E ⁶	76	74.3	74	71.3	67	69.1	34	40.4	27	29.2	25	24.7
E ⁷	0	0.0	0	0.0	0	0.0	0	0.0	0	0.0	0	0.0

FRQ set in italics: estimated frequencies according to OHRENDORF and HAEUSELER

Table VII: Observed (FRQ) and with the short range model SR IV calculated (FRC) frequencies of 6 Chalcogenides with Chalcopyrite structure (in cm^{-1})

B_1^3 are systematically higher and for mode B_1^2 lower than the experimental ones, which means that the calculated splitting between modes B_1^1 and B_1^2 is by ca. 8cm^{-1} wider than observed in the experiments. But this result should not be overestimated as the frequencies of species B_1 are unsure in the most cases and even are missing in others.

As can be seen from table IX, the force constants obtained for the 12 chalcopyrite compounds show some characteristic trends. The ratio K_1/K_2 is found to be 1/2 in the case of the chalcogenides while it is 2/3 for the pnictides. This finding may be explained by the different ratios of the formal charges of the cations involved which is 1:3 in the case of the

ΔF	ZnSiP ₂		ZnGeP ₂		CdSiP ₂		CdGeP ₂		CdSnP ₂		CdGeAs ₂	
	FRQ	FRC	FRQ	FRC	FRQ	FRC	FRQ	FRC	FRQ	FRC	FRQ	FRC
A ₁	337	341.6	328	332.7	326	327.6	321	322.7	301	300.6	196	194.3
A ₂		382.6		356.7		365.3		348.5		330.9		203.8
A ₂		336.2		322.1		307.6		297.0		288.2		183.3
B ₁ ¹	484	492.3	389	389.0	462	476.9	373	372.1	330	332.8	260	261.5
B ₁ ²	335	324.0	247	241.6	315	303.6	225	220.5	165	164.5	165	167.3
B ₁ ³	130	134.2	120	129.9	88	84.9	85	85.3	80	83.0	75	73.4
B ₂ ¹	494	494.7	397	394.2	486	486.5	387	387.9	353	349.8	273	274.9
B ₂ ²	342	343.4	340	337.3	306	308.5	295	293.3	288	286.2	205	204.7
B ₂ ³	145	150.7	120	119.2	109	117.9	88	90.3	73	76.2	73	78.7
B ₂ ⁴	0	0.0	0	0.0	0	0.0	0	0.0	0	0.0	0	0.0
E ¹	494	494.1	386	387.2	486	485.2	385	382.5	340	343.2	275	272.5
E ²	462	457.8	370	370.0	454	449.3	354	354.4	314	313.8	259	259.4
E ³	327	322.2	330	328.2	284	282.7	289	286.8	280	280.9	203	202.9
E ⁴	264	276.8	203	211.0	252	262.3	179	189.5	146	147.0	160	159.0
E ⁵	184	180.4	141	141.6	156	151.5	121	115.4	93	91.7	96	91.3
E ⁶	102	98.0	94	84.9	66	66.4	63	61.4	54	52.1	46	45.8
E ⁷	0	0.0	0	0.0	0	0.0	0	0.0	0	0.0	0	0.0

FRQ set in italics: estimated frequencies according to OHRENDORF and HAEUSELER

Table VIII: Observed (FRQ) and with the short range model SR IV calculated (FRC) frequencies of 6 Pnictides with Chalcopyrite structure (in cm⁻¹)

chalcogenides and 2:4 for the pnictides pointing to a more covalent bonding in the pnictides. The same result is obtained from a comparison of the force constants K_1 and K_2 for chalcogenides and pnictides of similar masses, for instance CuAlS₂/ZnSiP₂, which shows that both constants exhibit higher values in the case of the pnictides. Both the values of K_1 and K_2 decrease with increasing mass of the B-cation which is due to the increasing lattice parameters and therefore atomic distances (see table I) with the ionic radii of the metal ions which normally increases with the mass.

Remarkable are the relatively high values of force constant F32, which correspond to the interaction of the B-cations. Surely this is not a hint to metal-metal bonding but is due to Coulomb repulsion between the two ions of equal charge. Accordingly the values of F32 become smaller with increasing mass of the anion, as one can assume that i) with increasing main quantum number of the anion the ionicity of the compounds decreases, i.e. the charge of the cations become smaller, and ii) the distances between the cations become wider.

	K1	K2	H2	F1	F32	F31	F33	k
CuAlS ₂	0,528	1,121	0,054	0,083	0,179	-0,007	-0,007	-0,088
CuGaS ₂	0,509	1,128	0,028	0,101	0,241	-0,012	-0,012	-0,040
CuInS ₂	0,449	1,059	0,000	0,082	0,249	0,006	0,006	-0,022
AgGaS ₂	0,490	1,142	0,017	0,062	0,277	-0,019	-0,019	-0,047
AgGaSe ₂	0,504	0,910	0,057	0,024	0,189	-0,014	-0,014	-0,090
AgInSe ₂	0,437	0,847	0,002	0,059	0,247	-0,024	-0,024	-0,045
ZnSiP ₂	0,835	1,356	0,083	0,100	0,298	0,010	0,010	0,007
ZnGeP ₂	0,895	1,289	0,062	0,074	0,292	0,011	0,011	-0,022
CdSiP ₂	0,797	1,296	0,077	0,070	0,289	0,000	0,000	-0,034
CdGeP ₂	0,832	1,227	0,045	0,064	0,270	0,003	0,003	-0,038
CdSnP ₂	0,768	1,141	0,038	0,056	0,173	-0,005	-0,005	-0,001
CdGeAs ₂	0,794	1,077	0,057	0,042	0,066	-0,003	-0,003	-0,040

Table IX: Force constants (N/cm) for chalcopyrite-type compounds (model SR IV)

All the other force constants show only small values which are below 0.1 N/cm. Nevertheless they are needed to adjust especially the modes in the low wavenumber region of the spectrum.

A direct comparison of the force constants obtained by our calculation with those given in the literature is not possible as most of the calculations done in the literature are performed using a rigid ion model. This should lead to different values for the short range force constants. But nevertheless also in these results the B-X stretching force constants are higher than the A-X constants, the stretching force constants for the pnictides are higher than those of a chalcogenide with similar masses, and the FAX/FBX ratio is comparable to the one found in this paper. (To obtain similar values for the stretching force constants calculated by the Keating model and by the Urey Bradley the Keating model parameters have to be multiplied by 3, as has been shown by OHRENDORF by a comparison of the definition of the internal co-ordinates in both models. For the deformation constants the connection between both models is not so straightforward.)

The normal co-ordinates and the potential energy distribution for the lattice vibrations of the chalcopyrite compounds are shown in fig. 2 and 3 in the form of bar diagrams of the mean values over all 12 compounds. As the normal co-ordinate of species A₁ consists of SC1 only it is omitted here as are the translational motions in species B₂ and E.

As can be seen from the standard deviations shown in fig. 2 the normal co-ordinates of the chalcopyrites under investigation are very similar as we already claimed in our previous paper. The same holds for the potential energy distribution shown in fig. 3 though in this case the standard deviations are a bit higher especially for instance for the force constant K1 in the mode B₁³ or for F1 in the mode E⁶. But nevertheless these data show clearly the close relationship of the lattice dynamics of pnictide and chalcogenide chalcopyrites.

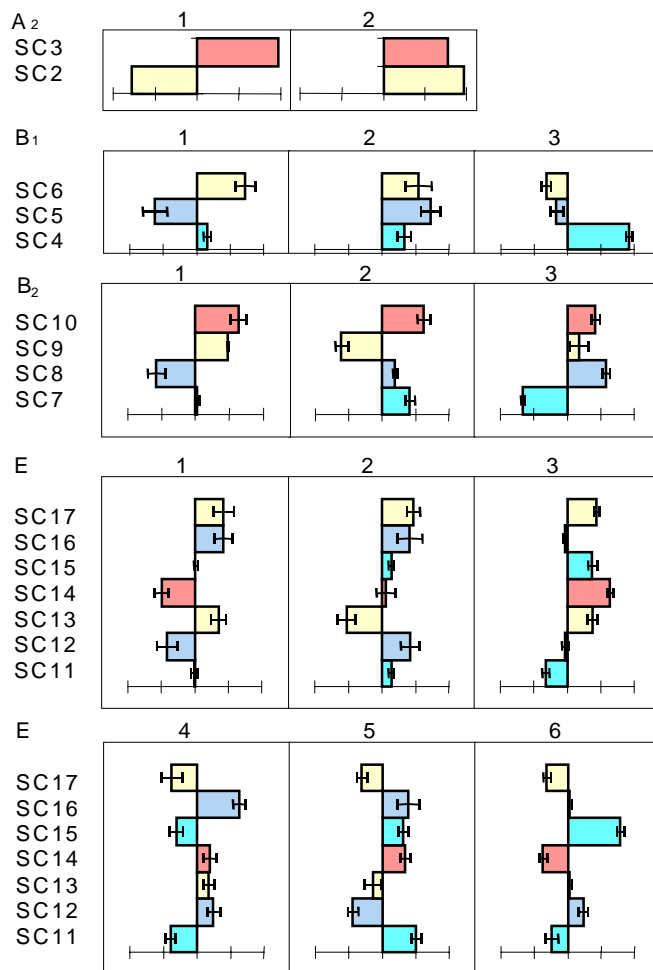


Fig. 2: Normal co-ordinates for chalcopyrite-type compounds calculated with model SR IV (mean values over 12 compounds)

For the two silent modes of species A₂ the normal co-ordinates are the sum and the difference of the two corresponding symmetry co-ordinates SC2 and SC3. From the point of view of the PED A₂¹ can be regarded as a characteristic vibration of the B-X sublattice while in the mode A₂² the potential energy is mainly located in the AX force constant K1 of course, but there are also relatively high values for the bending co-ordinate H1 and the second nearest neighbour interactions F1 and F2.

The modes B₁¹ and B₁² mainly are vibrations of the B-X sublattice, namely a stretching and a bending vibration, respectively. The participation of the A-cation in these vibrations is only relatively small. This is supported by the relatively high value for K2 in the PED obtained for B₁¹. B₁² on the other hand though mainly a vibration of the B-X sublattice as well shows a small participation of K2 only but high values for the force constant K1 and for the interaction of B cations in the unit cell. The mode B₁³ on the other hand is nearly a vibration of the A-cations only combined with small evasive movements of the anions and the B-cations only which is also shown by the high value for K1 in the PED of this mode.

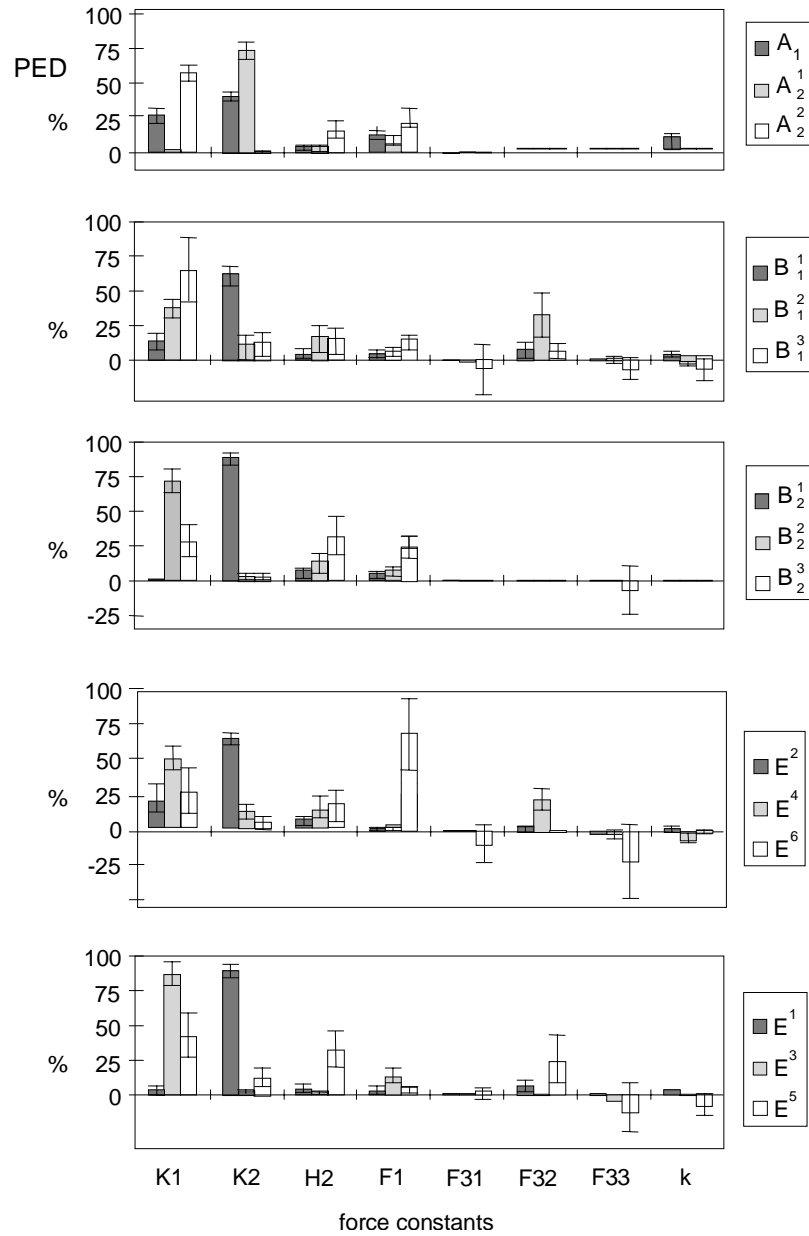


Fig.3: Potential energy distribution (PED) for the zone centre modes of the chalcopyrite lattice calculated by the short range model SR IV (mean values over 12 compounds)

In species B₂ the mode of highest wavenumber is once again mainly a vibration of the B-X sublattice with nearly 90% of the potential energy located in the force constant K2. In B₂² both cations vibrate against the anion sublattice in z-direction but the main part of the potential energy is located in the AX-bond while in B₂³ the B-X sublattice moves against the

A-cations with the major part of the potential energy in the bending co-ordinates and next nearest neighbour interaction constants.

For species E the situation is more complicated, as there are 7 independent symmetry co-ordinates which may be linearly combined to form the normal co-ordinates. But especially for the modes of high wavenumber there are some clear trends: E^1 is a B-X vibration only, the symmetry co-ordinates of the A-cations SC11 and SC15 are not involved in this vibration. This is also shown by the high value for K2 in the PED of this mode. E^3 on the other hand is an A-X vibration with no participation of the B-cations (SC12 and SC16) and the potential energy mainly located in the A-X-bond. E^2 can be compared both from the point of the normal co-ordinates and from the PED with B_2^2 as it is as well a vibration of the cations against the anion sublattice but this time in the xy-plane. During all the modes E^4 , E^5 and E^6 the A and B-cations move against each other in the xy-plane but with increasing participation of the A-cations for the modes with lower wavenumbers. Unique in the PED is the very high value for the interaction of the A cation in the unit cell obtained for the mode E^6 . This surely is not due to covalent bonding between these two ions of equal charge but to Coulomb repulsion. This has to be checked by calculations including charges on the different ions.

References

- ABRAHAMS C., BERNSTEIN J.L., J. Chem. Phys. **52**, 5607-5613 (1970).
 ABRAHAMS C., BERNSTEIN J.L., J. Chem. Phys. **55**, 796-803 (1971).
 ARTUS L., PASCUAL J., PUJOL J., CAMASSEL J., FEIGELSON R. S., Phys. Rev. **B 43**, 2088 (1991).
 ARTUS L., PUJOL J., PASCUAL J., CAMASSEL J., Phys. Rev. **B 41**, 5727 (1990).
 ARTUS L., PASCUAL J., J. Phys. Condensed Matter **4**, 5835 (1992).
 BENOIT P., CHARPIN P., LESUEUR R., DJAGA-MARIADASSOU C., in Proc. Fourth Intern. Conf. on Ternary and Multinary Semiconductors, Tokyo, 1980.
 BETTINI M., Phys. Stat. Sol. **B 69**, 201 (1975).
 HOLAH G.D., WEBB J.S., MONTGOMERY H., J. Phys. C: Solid State Phys. **7**, 3875 (1974).
 KAMINOV I.P., BUEHLER E., WERNICK J.H., Phys. Rev. **B 2**, 960 (1970).
 KOSCHEL W. H., BETTINI M., Phys. Stat. Sol. **B 72**, 729 (1975).
 LAUWERS H. A., HERMAN M. A., J. Phys. Chem. Solids **38**, 983 (1977).
 NEUMANN H., Cryst. Res. Technol. **24**, 619 (1989).
 OHRENDORF F. W., HAEUSELER H., Cryst. Res. Technol. **34**, 339 (1999).
 OHRENDORF F.W., PhD thesis, University of Siegen, (1997).
 PASCUAL J., PUJOL J., ARTUS L., CAMASSEL J., Phys. Rev. **B 43**, 9831 (1991).
 POPLAVNOI A. S., TYUTEREV V. G., J. Phys. Colloque **C3**, 169 (1975).
 KOPYTOV A.V. AND POPLAVNOI A. S., Sov. Phys. Journal **23**, 353 (1980).
 SPIES H.W., HAEBERLEN V., BRANDT G., RÄUBER A., SCHNEIDER J., Phys. Stat. Sol. **B62**, 183 (1974).
 VAIPOLIN A.A., Fiz. Tverd. Tela **15**, 1430 (1973).

(received May 7, 1998; accepted June 18, 1998)

Authors' address:

Dr. F.W. OHRENDORF and Prof. Dr. H. HAEUSELER
 Laboratorium für Anorganische Chemie
 Universität-GH Siegen
 D-57068 Siegen
 e-mail: haeuseler@chemie.uni-siegen.de